

# Comparing wind turbine aeroelastic response predictions for turbines with increasingly flexible blades

Kathy Cao<sup>1</sup>, Kelsey Shaler<sup>2</sup>, Nick Johnson<sup>2</sup>

<sup>1</sup> Johns Hopkins University, Baltimore, MD, USA

<sup>2</sup> National Renewable Energy Laboratory, Golden, CO, USA

Author contact email: [kathy.cao8438@gmail.com](mailto:kathy.cao8438@gmail.com)

Keywords: Free Vortex Wake, turbine wakes, turbine modeling, flexible blades

**Abstract.** Highly flexible blades are becoming more prevalent designs as a potential solution to the transportation challenges associated with large-scale wind turbine rotors. However, there is currently no quantitative definition of “highly flexible” blades. To further develop turbines with highly flexible blades, a precise definition of the term and accurate simulations of turbines with such blades are required. Assumptions made in the traditional aerodynamic model, Blade Element Momentum (BEM) theory, are violated in turbines with flexible blades. However, Free Vortex Wake (FVW) methods can more accurately model these turbine designs. Though more computationally expensive than BEM, FVW methods are still computationally tractable for use in iterative turbine design. The purpose of this work was to determine the blade flexibility at which BEM and FVW methods begin to produce diverging aeroelastic response results. This was accomplished by simulating the BAR-DRC reference turbine with increasingly flexible blades in a range of steady, uniform inflow conditions using OpenFAST, the National Renewable Energy Laboratory’s physics-based turbine engineering tool. Blade-tip deflections confirmed that BEM and FVW results diverge as blade flexibility increases. For the 212 m rotor diameter turbine used in this study, the two methods largely agreed for smaller blade deflections. But their results differed by an average of 5% when the out-of-plane blade-tip deflections exceeded 5% of the blade length and in-plane blade-tip deflections exceeded 1.25% of the blade length, with percent differences approaching 25% at the largest deflections.

## 1. Introduction

Modern-day wind turbines can generate twenty times the energy of turbines first developed in the 1990s, making wind energy competitive in the global energy market [1]. This progress is partially due to technological developments enabling larger turbine rotors with increasingly longer blades [1]. Large-scale rotors increase energy generation capacity by increasing rotor-swept areas and decreasing the minimum wind speed for power generation. However, these large-scale rotors are difficult to transport due to their size [2].

Specifically, rail transportation of larger blades must be able to accommodate bends with up to 13-degree lateral curves [3] in the tracks without the blades suffering structural damage. These curves limit current blades to 75 meters long, but large-scale rotors can have blades upwards of 100 meters long [2].



Highly flexible blades are a potential solution to this challenge, having shown potential with controlled bending of 100-meter-long blades in rail transport [2].

Due to the iterative nature of wind turbine design, simulations have become a common tool in the design process of turbines. As researchers push the bounds on blade flexibility, they need accurate computational modeling software to understand how highly flexible blades perform in the field. However, highly flexible blades violate assumptions made in Blade Element Momentum (BEM) theory, the standard aerodynamic model used for turbine design. For instance, BEM theory makes actuator-disk assumptions that are violated when blades deflect outside of the rotor plane. Such large out-of-plane deflections also cause complexities in the near wake that are not accounted for in BEM theory.

Although highly flexible blades and other complex turbine designs or inflow conditions may be modeled using Computational Fluid Dynamic (CFD) models with higher accuracy, CFD models are too computationally expensive to feasibly be used in iterative design and load analysis processes. Free Vortex Wake (FVW) methods offer a compromise between lower-fidelity models such as BEM and higher-fidelity models such as CFD [4]. FVW methods are mid-fidelity models that can simulate complex physics while requiring reasonable computational resources for the iterative turbine design process.

FVW models have been studied for several decades. Early work from Rosenhead discusses the formation of elemental vortices from “surfaces of discontinuity” [5]. In a later work, Winckelmans and Leonard also present contributions to vortex particle methods [6]. More recently, Papadakis’ work combines standard Eulerian CFD methods with Lagrangian vortex particle methods in a hybrid CFD methodology [7].

Existing FVW modelling codes for wind turbines include the vortex particle approach of GENUVP [8] and vortex filament approach of AWSM [9]. Branlard expanded on previous works to use FVW methods in aeroelastic wind turbine modeling in sheared and turbulent inflow conditions [10]. This work focuses on the recently implemented FVW model in OpenFAST, the National Renewable Energy Laboratory’s physics-based wind turbine engineering tool. The model, called cOnvecting LAGrangian Filaments (OLAF), uses a hybrid lattice/filament method, further explained in section 3.1.

Previously, BEM was the only aerodynamic modeling option in OpenFAST. OLAF was implemented as an alternative aerodynamic model for instances where higher fidelity simulations are required, such as for turbines with highly flexible blades [11]. It should be noted that although FVW methods have been shown to more accurately model flexible blades [4], there is currently no quantitative definition of “highly flexible” blades.

## 2. Objectives

The goal of this work was to establish when blade flexibility exceeds the limits of standard BEM models and requires the use of the higher-fidelity aerodynamic models, such as FVW models. This was accomplished by comparing the aeroelastic response predictions from BEM and FVW for turbines with increasingly flexible blades, and in doing so, determine at what flexibility the results from the models diverge. These results may be used in developing a more precise definition of “highly flexible” blades in the context of BEM and FVW methods. Having such a definition will be instrumental in accurately modeling turbine performance for the iterative design of future turbines. Additionally, recommendations from this study can give insight into the necessity of using FVW methods as opposed to BEM in OpenFAST for blade design, highlighting FVW methods’ importance in the field of turbine modelling.

## 3. Methodology

### 3.1. Overview of OpenFAST and OLAF

OpenFAST is a simulation tool that couples modules for aerodynamics, hydrodynamics for offshore turbines, control and electrical system dynamics, and structural dynamics. With these modules, OpenFAST solves the aero-hydro-servo-elastic dynamic responses of individual wind turbines [11].

Simulations were run with OpenFAST v3.0.0., using the BEM and OLAF aerodynamic modeling options in *AeroDyn15* [11]. The integration of the two models in *AeroDyn15* is shown in Figure 1.

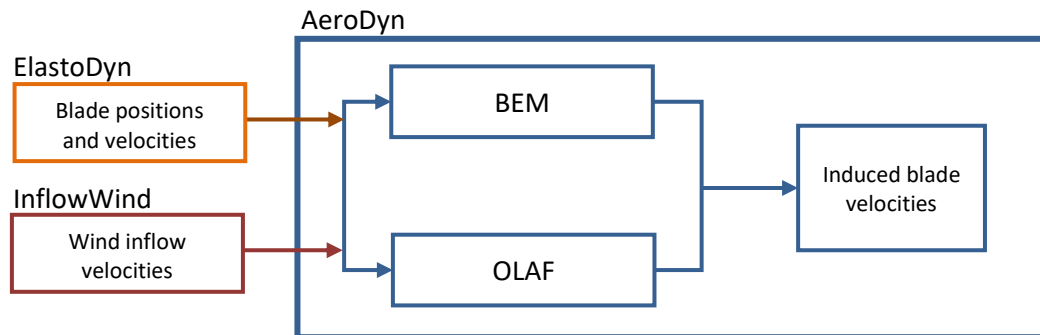


**Figure 1.** OLAF and BEM integration with *AeroDyn15* [11]. Inputs from *ElastoDyn* and *InflowWind* modules.

Generally, in FVW methods, the turbine wake is discretized into Lagrangian markers, defined in terms of wake age and azimuthal blade location [11]. There are many FVW methods with various wake discretization methods. In OLAF, a lattice is used to represent the near wake and straight-line filaments are used to represent the far wake [11], as shown in Figure 2.

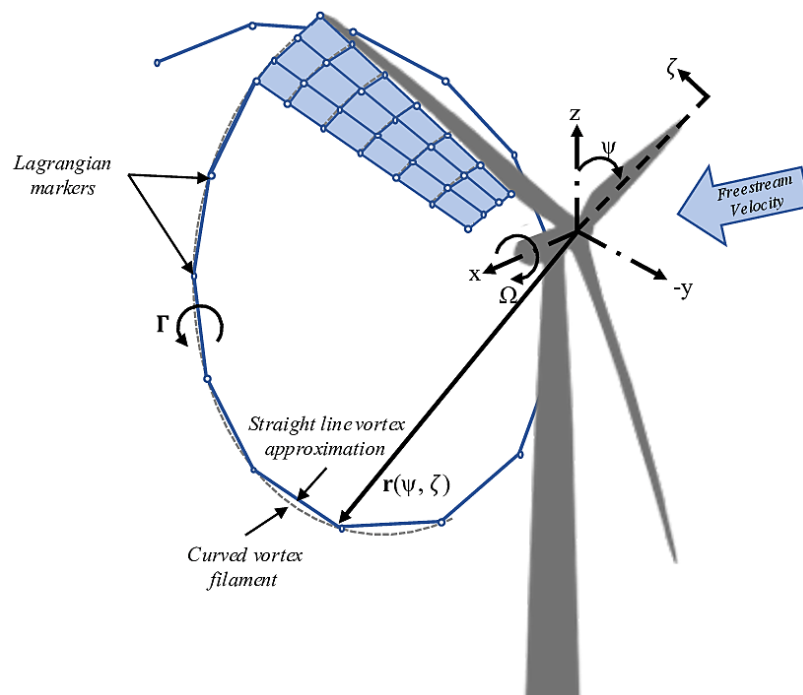


**Figure 2.** Evolution of near-wake lattice, blade tip vortex, and Lagrangian markers in OLAF [11].

### 3.2. Simulation cases

The reference BAR-DRC turbine used in this work was developed for the Big Adaptive Rotor (BAR) project [2]. The BAR-DRC, is a Downwind turbine with blades designed to be transported by Rail and made of pultruded Carbon fiber laminate. The BAR-DRC is a large-scale, highly flexible turbine with a rotor diameter of 212 m. To ensure consistent operation between BEM and OLAF simulations, rotor

speed and blade pitch were kept constant and specified based on the inflow wind speed, as described in Figure 3. No controller was used.

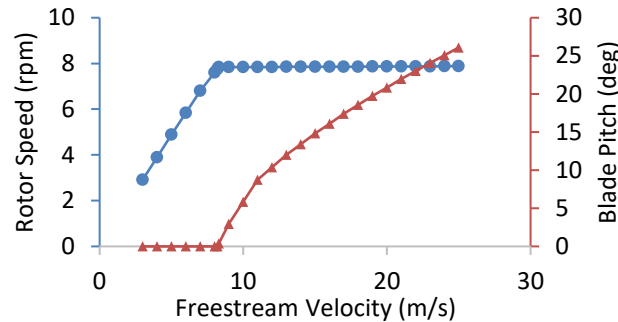


Figure 3. Turbine operation of BAR-DRC [2].

For this study, input parameters in the *InflowWind*, *AeroDyn*, and *ElastoDyn* modules were varied, as detailed in Figure 4. The tower shadow model was on in *AeroDyn* and OLAF, indicating that the influence of the tower on the windstream and wake convection would be computed. Horizontal wind speed was varied from 4 m/s to 18 m/s in the *InflowWind* module with steady, uniform inflow. The aerodynamic model was varied between BEM or OLAF in the *AeroDyn* module. The blade stiffness and damping factors were varied independently between 0.1 and 5.0 in the *ElastoDyn* module. While one factor was varied, the remaining stiffness factors and structural damping parameters were held constant at 1.0 and 3.0, respectively. The blade stiffness factors and damping factors are ratios of the stiffness and damping values to those initially specified in the blade input files.

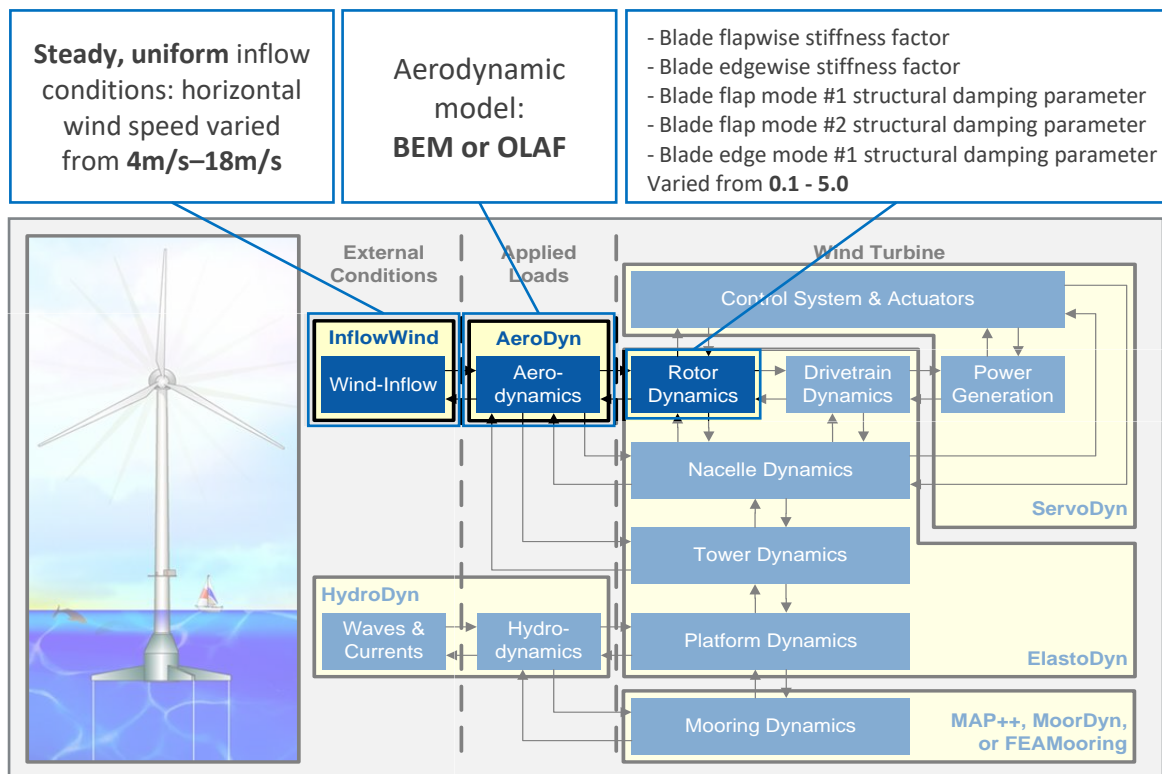


Figure 4. OpenFAST structure [11]. Callouts show variables for different simulation cases.

Several input parameters in the OLAF module were set based on wind speed according to discretization and regularization studies [11]. The discretization parameters were used to determine the number of FVW time steps for which to compute the lattice for the near wake and straight-line filaments for the far wake.

**Table 1.** Discretization and regularization values for OLAF module.

Parameter		Value
For discretization	Wake discretization (deg)	5
	Near wake extent (rotor diameter, $D$ )	2
	Far wake extent ( $D$ )	5
For regularization	Wake regularization	1.164
	Wing regularization	1.048
	Core spread	5350

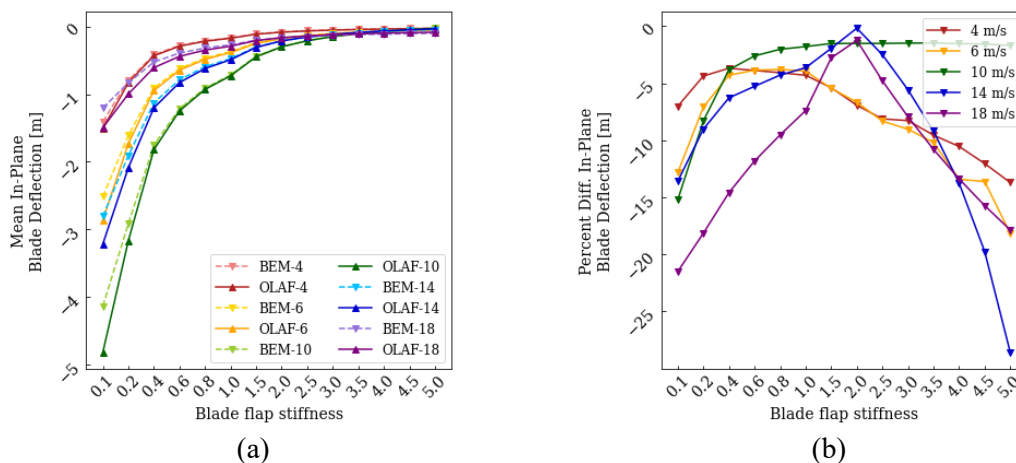
Each simulation case ran for 1200 seconds of simulation time, ensuring convergence of all results. Initial transients were not considered in the analysis, and results were evaluated from 600 to 1200 seconds. Output parameters included rotor torque, rotor power, rotor thrust, blade-tip deflections, blade-root bending and pitching moments, tower deflections, tower-top and tower-base bending and yaw moments, and low-speed shaft bending moments. This paper focuses on blade-tip deflections and rotor torque.

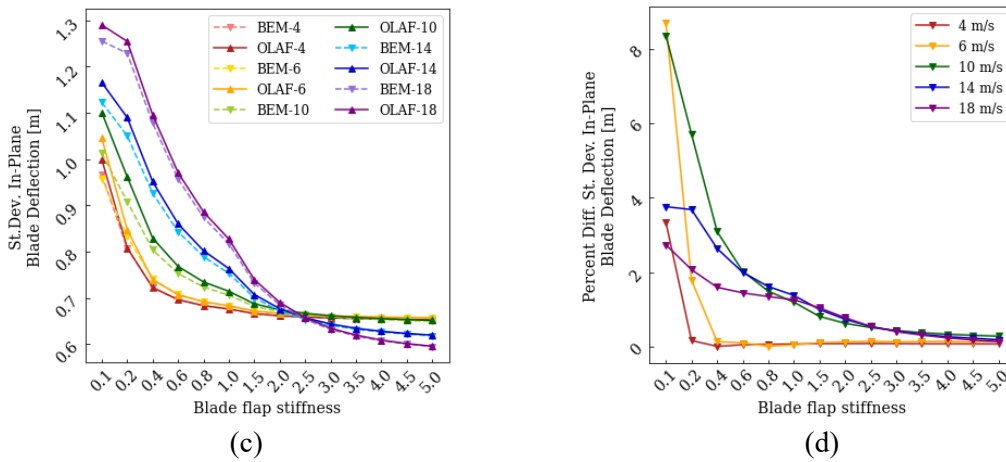
## 4. Results

### 4.1. Simulation results

The mean and standard deviations of the time series results were compared between codes and for varying stiffness and damping factors. Percent differences between the code results are also considered.

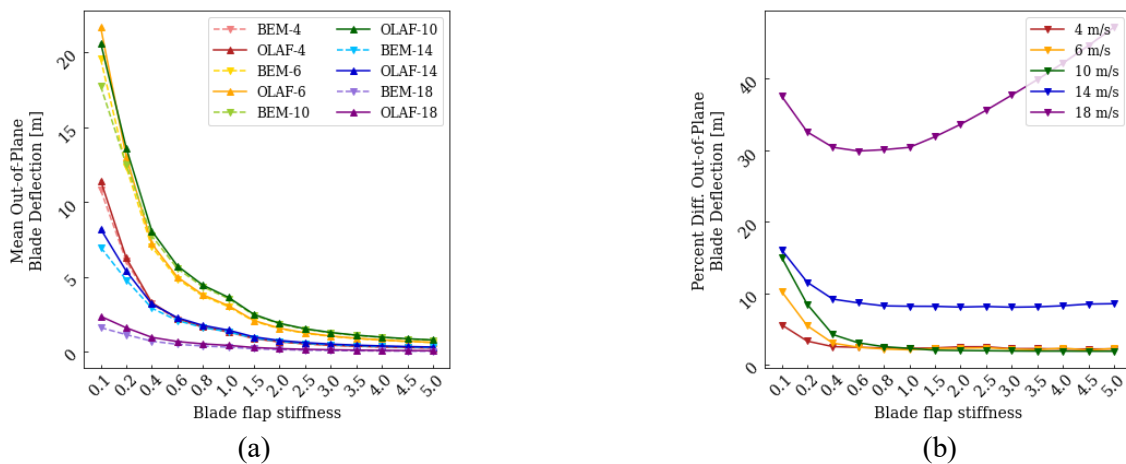
Figure 5 shows the time averages, standard deviations, and respective percent differences between results from BEM and OLAF for in-plane blade-tip deflections over varied blade flapwise stiffness. As seen in Figure 5a, the greatest in-plane blade deflection was obtained at the lowest blade flapwise stiffness value. Additionally, as the blade flapwise stiffness increased, the deflection for both BEM and OLAF simulations approached 0 m. The percent differences between BEM and OLAF mean in-plane deflections tended to be greater for cases with lower flapwise stiffness values, with several cases exceeding a 5% difference between BEM and OLAF means, as shown in Figure 5b. As shown in Figure 5c, BEM and OLAF standard deviations decreased as blade flapwise stiffness increased for in-plane blade-tip deflections. As shown in Figure 5d, the percent differences between BEM and OLAF standard deviations exceeded 5% for some cases at the lowest blade flapwise stiffness as well.





**Figure 5.** Time averages and standard deviations of in-plane blade-tip deflections and percent differences between BEM and OLAF results for varying blade flapwise stiffness factor. Inflow wind speeds are designated with line color and computational method is designated with line style. Note that percent differences are artificially increased for cases with means or standard deviations near 0 m.

Figure 6 shows results for out-of-plane blade-tip deflections over varied blade flapwise stiffness, which had similar trends to the in-plane deflections. As seen in Figure 6a, the greatest out-of-plane deflection was also obtained at the lowest blade flapwise stiffness value, with deflections approaching 0 m as the stiffness increased. As shown in Figure 6b, the percent differences between BEM and OLAF mean out-of-plane deflections exceeded 5% for many cases. Additionally, the standard deviations decreased as blade flapwise stiffness increased, as shown in Figure 6c. The percent differences between the standard deviations were greater for lower flapwise stiffness values, as shown in Figure 6d.



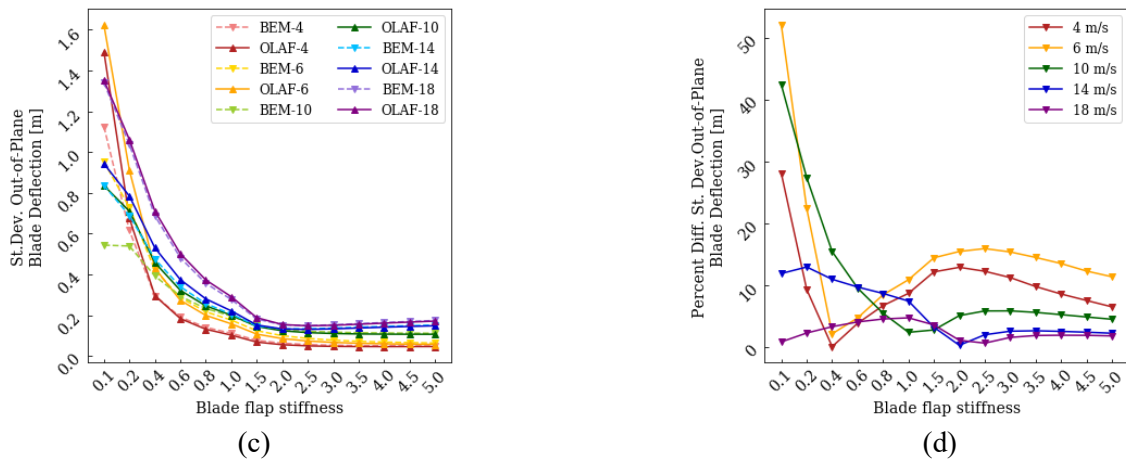


**Figure 6.** Time averages and standard deviations of out-of-plane blade-tip deflections and percent differences between BEM and OLAF results for varying blade flapwise stiffness factor. Inflow wind speeds are designated with line color and computational method is designated with line style. Note that percent differences are artificially increased for cases with means or standard deviations near 0 m.

Varying the blade flapwise stiffness factor had a significantly greater effect on the blade-tip deflections than varying the blade edgewise stiffness factor and the three blade damping parameters. Hence, due to space limitation, these results are not shown.

In general, in-plane and out-of-plane blade-tip deflections decreased in magnitude as blade stiffness increased. Additionally, blade-tip deflection results from OLAF were generally greater in magnitude than those from BEM, with the difference between the results increasing for more flexible blades. Maximum mean blade-tip deflection values are shown in Table 2. For the BAR-DRC turbine, this maximum out-of-plane blade-tip deflection is equivalent to 21.4% of the blade length and likely violates assumptions made in BEM theory regarding a 2D rotor plane. These results suggest that BEM and OLAF results deviate to a higher degree as blades become more flexible.

**Table 2.** Maximum mean blade-tip deflection results, obtained from OLAF for the case at 0.1 blade flapwise stiffness factor with 6 m/s inflow wind speed.

Direction	Mean deflection (m)
Out-of-plane	21.66
In-plane	4.82

Other parameters, such as out-of-plane blade-root bending moment, confirm these deviations between BEM and OLAF results for highly flexible blades. Similar to the out-of-plane blade deflection results, the out-of-plane blade-root bending moment percent differences of the means were higher for lower values of blade flapwise stiffness, many exceeding 5% with a maximum of 14% difference between BEM and OLAF results. These results for the out-of-plane blade-root bending moment emphasize that BEM and OLAF results agree for stiffer blades while deviating for more flexible blades and that the turbine’s loads are affected by varying blade flexibility. These variances would have a large impact on the design of wind turbine blades.

#### 4.2. Non-dimensionalized results

To determine the values of in-plane or out-of-plane blade deflections at which BEM and OLAF results begin to diverge, the time-averaged rotor torque results from each model were non-dimensionalized from hub-height inflow wind velocity and plotted against the blade deflections.



BEM and OLAF results were processed independently. The time-averaged data from cases where blade edgewise stiffness and flapwise stiffness were used in this analysis while the data from cases where blade damping factors were omitted.

To non-dimensionalize the torque data, the data was first binned by deflection value and grouped by wind speed in each bin. Then, each torque data point was divided by the mean of the torque values in the first bin and respective wind speed group. After non-dimensionalizing each individual torque value, the mean torque for each bin was calculated and plotted against the bins' boundary values, as shown in Figure 7.

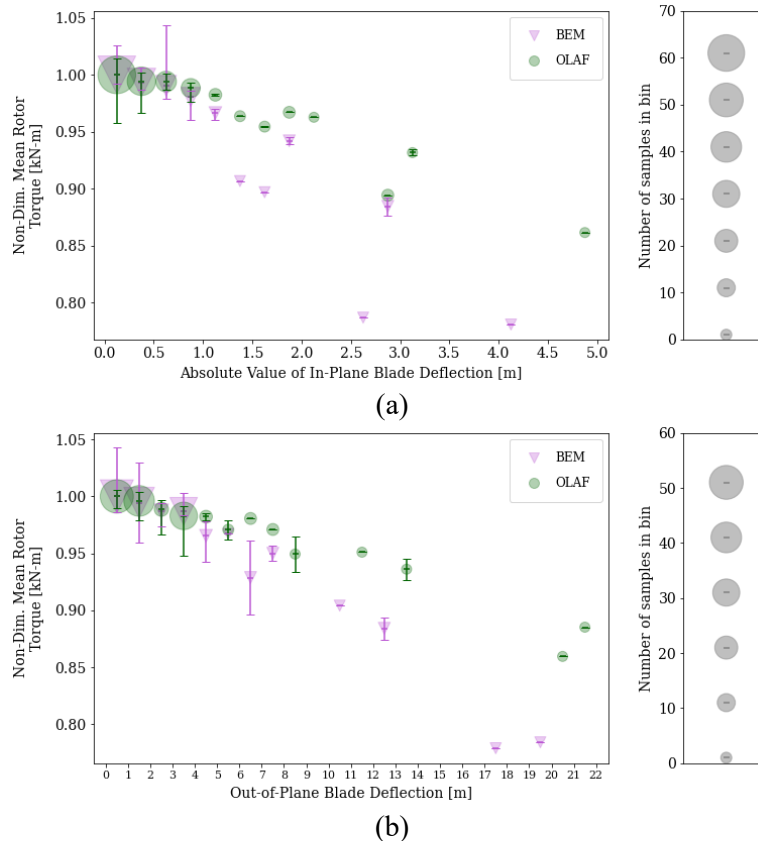


**Figure 7.** Non-dimensionalized time-averaged rotor torque vs. binned (a) out-of-plane and (b) in-plane blade-tip deflection results from BEM and OLAF. Binned results include data from varied blade stiffness factor cases. Horizontal markers represent bin means, and error bars represent minimum and maximum non-dimensionalized values in each bin.

To determine specific in-plane and out-of-plane deflection values for which the deviation between BEM and OLAF was significant, percent differences between the bin means were calculated for several output parameters, including rotor torque, rotor power, rotor thrust, blade deflections and bending moments, and tower deflections and bending moments.

The percent difference could not be calculated for bins associated with larger deflection values since the BEM and OLAF bins had one or no points. Hence, to get a better perception of the maximum deviation between the non-dimensionalized results from BEM and OLAF, percent differences were calculated between the points in the largest bins for BEM and OLAF, regardless of if they were in the same bin.

For smaller deflection values, the non dimensionalized results from BEM and OLAF were largely consistent with each other, with percent differences between 0% and 5%. However, percent differences



approached 25% for non-dimensionalized data binned by out-of-plane blade-tip deflection and 13% for non-dimensionalized data binned by in-plane blade-tip deflection. Generally, the percent difference between the non-dimensionalized results from BEM and OLAF exceeded 5% when the out-of-plane blade-tip deflection exceeded 5 m or when the in-plane blade-tip deflection exceeded 1.25 m.

These results provide a greater understanding of when BEM and FVW modeling approaches predict significantly different results when modeling highly flexible blades, and thus a more precise definition of “highly flexible” blades in the context of BEM and FVW methods.

## 5. Conclusions and future work

In this work, aeroelastic response predictions from OLAF—a recently implemented FVW model in the turbine modeling tool OpenFAST—were compared to those from the standard lower-fidelity BEM model.

The blade stiffness was modified, resulting in out-of-plane and in-plane blade-tip deflections ranging from 0 – 21.66 m (0 – 21.4% of the blade length) and 0 – 4.82 m (0 – 4.7% of the blade length), respectively. In general, the smaller out-of-plane and in-plane blade-tip deflections’ means and standard deviations of FVW results were consistent with BEM results, with percent differences less than 5%. Though FVW methods may certainly be used for less flexible blades, the more computationally efficient BEM method is adequate for modeling these turbines under steady, uniform inflow conditions with no yaw misalignment.

Results from the FVW model began to deviate significantly from results from the BEM model for cases with in-plane and out-of-plane blade-tip deflections greater than 1.25 m (1.25% of the blade length) and 5 m (5% of the blade length), respectively. For these cases, the BEM method tended to under-predict load magnitudes compared to the FVW method, which has implications for blade designs and the levelized cost of energy.

At these conditions, the large blade-tip deflections violate assumptions made in BEM theory. Hence, this work recommends that FVW methods be used when in-plane blade-tip deflections exceed 1.25% of the blade length or when out-of-plane blade-tip deflections exceed 5% of the blade length. These values also provide preliminary guidance for defining “highly flexible” blades.

Further studies are needed to determine if these recommendations are dependent on blade length. This study was limited by one turbine configuration with approximately 100 m long blades. Hence, it is not certain if the same blade-tip deflection results and deviations between BEM and FVW results would be seen for turbines with other blade lengths.

Further work is also needed in comparing BEM and FVW simulations with turbulent inflow conditions, as opposed to steady inflow. Adding turbulence to the simulations would provide a more realistic depiction of turbines with highly flexible blades in the field. Turbulent inflow cases would also provide a basis for analysis of ultimate and fatigue loads, which are more impactful in the wind turbine design process.

## Acknowledgements

I would like to thank my mentor, Kelsey Shaler, for her guidance and support throughout my SULI experience. Her consistent encouragement and enthusiasm have helped me develop my technical skills and have inspired me to continue pursuing a career in renewable energy. I would like to extend my thanks to Nick Johnson and Emmanuel Branlard for their advice and feedback on this work.

This work was supported in part by the U.S. Department of Energy, Office of Science, Office of Workforce Development for Teachers and Students (WDTS) under the Science Undergraduate Laboratory Internship (SULI) program.

This work was authored in part by the National Renewable Energy Laboratory, operated by Alliance for Sustainable Energy, LLC, for the U.S. Department of Energy (DOE) under Contract No. DE-AC36-08GO28308. Funding provided by the U.S. Department of Energy Office of Energy Efficiency and Renewable Energy Wind Energy Technologies Office. The views expressed in the article do not necessarily represent the views of the DOE or the U.S. Government. The U.S. Government retains and

the publisher, by accepting the article for publication, acknowledges that the U.S. Government retains a nonexclusive, paid-up, irrevocable, worldwide license to publish or reproduce the published form of this work, or allow others to do so, for U.S. Government purposes.

The research was performed using computational resources sponsored by the Department of Energy's Office of Energy Efficiency and Renewable Energy and located at the National Renewable Energy Laboratory.

## References

- [1] Johnson N, Bortolotti P, Dykes K, Barter G, Moriarty P, Carron S, Wendt F, Veers P, Paquette J, Kelly C and Ennis B. Investigation of innovative rotor concepts for the big adaptive rotor project. Technical Report NREL/TP-5000-73605. National Renewable Energy Laboratory, Golden, CO, September 2019.
- [2] Bortolotti P, Johnson N, Abbas N J, Anderson E, Camarena E and Paquette J. Land-based wind turbines with flexible rail-transportable blades—Part I: Conceptual design and aeroservoelastic performance. *Wind Energy Science*, 6:1277-90, 2021.
- [3] Carron WS and Bortolotti P: Innovative rail transport of a supersized land-based wind turbine blade, *J. Phys. Conf. Ser.*, 1618, 042041, 2020.
- [4] Shaler K, Anderson B, Martínez-Tossas T, Branlard E and Johnson N. Comparison of free vortex wake and BEM structural results for highly flexible turbines under challenging inflow conditions. *Wind Energy Science Discussions*, January 2022.
- [5] Rosenhead L. The formation of vortices from a surface of discontinuity. *Proc. of the Royal Society of London. Series A, Containing Papers of a Mathematical and Physical Character*, 134 (823):170-92, 1931.
- [6] Winckelmans GS and Leonard A. Contributions to vortex particle methods for the computation of three-dimensional incompressible unsteady flows. *Journal of Computational Physics*, 109(2):247-73, 1993.
- [7] Papadakis G. Development of a hybrid compressible vortex particle method and application to external problems including helicopter flows. Thesis. National Technical University of Athens, Aerodynamics Laboratory, December 2014.
- [8] Voutsinas SG. Vortex methods in aeroneutics: how to make things work. *International Journal of Computational Fluid Dynamics*, 20:3-18, 2006.
- [9] van Garrel A. Development of a wind turbine aerodynamics simulation module. Technical Report ECN-C-03-079. Energy Research Centre of the Netherlands, Petten, Netherlands, August 2003.
- [10] Branlard E, Papadakis G, Gaunaa M, Winckelmans G and Larsen TJ. Aeroelastic large eddy simulations using vortex methods: unfrozen turbulent and sheared inflow. *J. Phys.: Conf. Ser.*, 625: 012019, 2015.
- [11] Shaler K, Branlard E, and Platt A. OLAF User's Guide and Theory Manual. Technical Report NREL/TP-5000-75959. National Renewable Energy Laboratory, Golden, CO, June 2020.